Polymer 49 (2008) 2678–2685

Contents lists available at ScienceDirect

Polymer

journal homepage: www.elsevier.com/locate/polymer

Effectual drug-releasing porous scaffolds from 1,6-diisocyanatohexane-extended poly(1,4-butylene succinate) for bone tissue regeneration

Parintorn Hariraksapitak [a,1], Orawan Suwantong [a], Prasit Pavasant [b], Pitt Supaphol [a,*]

[a] The Petroleum and Petrochemical College, Chulalongkorn University, Bangkok 10330, Thailand
[b] Department of Anatomy, Faculty of Dentistry, Chulalongkorn University, Bangkok 10330, Thailand

ARTICLE INFO

Article history:
Received 29 November 2007
Received in revised form 2 April 2008
Accepted 5 April 2008
Available online 10 April 2008

Keywords:
Bone scaffolds
Solvent casting and particulate leaching
Poly(butylene succinate)

ABSTRACT

Tooth extraction induces residual ridge resorption which impairs function and aesthetic of dental prostheses. This study aimed at developing new bone scaffolds to be used in a tooth socket for preserving bone mass from the residual ridge resorption. Scaffolds were fabricated from poly(1,4-butylene succinate) extended with 1,6-diisocyanatohexane (PBSu–DCH) by solvent casting and particulate leaching technique. Four different weight ratios of NaCl particles (200–400 μm; used as the porogen species) and the polymer were varied (i.e., 25, 30, 35, and 40% based on the weight of the polymer). Scaffolds were evaluated for their physical (i.e., morphology, porosity, pore volume, and pore size), physico-mechanical (i.e., mechanical properties and water retention ability), and biological properties (i.e., cytotoxicity and bone cell attachment). The potential for use of the as-prepared materials as effectual drug-releasing scaffolds for bone tissue regeneration was assessed by incorporating ipriflavone and studying the release of the drug from the drug-loaded scaffolds.

1. Introduction

"Residual ridge" is a term used in dentistry to describe the shape of the clinical alveolar ridge existing after a complete healing of bone and soft tissues once a tooth had been extracted [1]. Improper shape or size of the residual ridge due to severe bone resorption diminishes dental prosthetic replacement to achieve aesthetic and function. Factually, resorption of the residual ridge is a chronically irreversible and cumulative mechanism [2]. It occurs continuously within the first year, with a particularly fast rate during the first 3–6 months [1,2]. The resorption continues at a slower pace throughout a life span, resulting in the removal of a large amount of jawbone. It was estimated that the bone loss occurred at ~21, ~36, and ~44% after a tooth had been extracted for 3, 6, and 12 months, respectively, and the alveolar bone may lose up to 10 mm of the lower jaw height after 25 years [1]. Prevention of the alveolar bone resorption caused by a tooth extraction, therefore, has been of great concern.

To preserve bone mass, various materials, e.g., autogenous or allogenic bone grafts [3], hydroxyapatite–collagen implant materials [4], and chemical agents like bisphosphonates [5,6], have been administered into the dental socket immediately after a tooth extraction. In the tissue engineering point of view, development of three-dimensional scaffolding biomaterials is a means for filling bone lesions [7]. Apart from the general characteristics of an ideal bone scaffold, a suitable scaffold for the dental socket should be soft, but mechanically strong enough to be easily placed in site without rupture or shape relapse. A synthetic biodegradable polyester is a material of choice due to its several promising properties. The gradual resorption behavior of this type of material is conducive to being concomitantly substituted with new bone mass [8]. Such a material can be tailored by a variety of fabrication methods to achieve the desired internal architecture that allows bone cells to move in and supports their attachment to the construct simultaneously [9,10].

Poly(1,4-butylene succinate) (PBSu) is an aliphatic biodegradable thermoplastic polyester, synthesized through a condensation polymerization of 1,4-butane diol and succinic acid. PBSu was proven to be biocompatible with osteoblasts, due to its ability in supporting both the proliferation and the differentiation of the cells [11]. However, with a melting temperature (T_m) in the range of 90–120 °C, PBSu with a low T_m is anticipated to possess an improved biodegradability. This could be achieved by an introduction of a certain type of non-crystallizable units into the polymer chains, which causes both the T_m and the crystallinity to decrease, when compared with those of the pure polymer [12]. 1,6-Diisocyanatohexane-extended PBSu (hereafter, PBSu–DCH) is one such modification that was developed by coupling PBSu with hexamethylene

* Corresponding author. Tel.: +66 2218 4131; fax: +66 2215 4459.
E-mail address: pitt.s@chula.ac.th (P. Supaphol).
[1] On study leave from the Department of Conservative Dentistry, Faculty of Dentistry, Prince of Songkla University, Hatyai, Songkhla 90112, Thailand.

0032-3861/$ – see front matter © 2008 Elsevier Ltd. All rights reserved.
doi:10.1016/j.polymer.2008.04.006

diisocyanate as a chain extender [13]. In the tissue engineering point of view, the properties of PBSu–DCH are expected to be improved over those of the pure PBSu and it is of our great interest to investigate whether PBSu–DCH is a suitable material for the preparation of scaffolds that enhance the regeneration of bone in the dental socket.

The present contribution focused on the fabrication of porous PBSu–DCH scaffolds by solvent casting and particulate leaching technique and the characterization of their properties pertinent to bone tissue regeneration. The effect of porogen/polymer weight ratio on architecture and characteristics of the as-prepared scaffolds was investigated. The potential for use of these scaffolds as carriers for delivery of an active substance suitable for enhancing bone tissue regeneration was investigated using ipriflavone (see Fig. I in Supplementary data for chemical structure), a synthetic derivative of isoflavone which has been known to accelerate osteoblastic activity and, at the same time, inhibits bone resorption [14], as the model compound.

2. Experimental section

2.1. Materials

Poly(1,4-butylene succinate) extended with 1,6-diisocyanatohexane (PBSu–DCH; pellet form; CAS number: 143606-53-5; batch number: 09717ED; melt index = 10 g/10 min at 190 °C/2.16 kg) and 7-(1-methylethoxy)-3-phenyl-4*H*-1-benzopyran-4-one or 7-isopropoxyisoflavone (hereafter, ipriflavone; CAS number: 35212-22-7; 97% purity) were purchased from Aldrich (USA). Chloroform (analytical reagent grade) was purchased from Labscan (Asia) (Thailand). Sodium chloride (NaCl; powder form) was purchased from Ajax Finechem (Australia). All other reagents were of analytical reagent grade and used without further purification.

2.2. Preparation of neat and ipriflavone-loaded PBSu–DCH scaffolds

Both the neat and the ipriflavone-loaded PBSu–DCH scaffolds were fabricated by the solvent casting and particulate leaching technique. First, PBSu–DCH pellets were dissolved in chloroform at 50 °C to obtain the PBSu–DCH solution at a fixed concentration of 15% w/v. The solution was left to cool down to room temperature. For the preparation of the drug-loaded scaffolds, ipriflavone (10% based on the weight of the polymer) was dissolved in the PBSu–DCH solution at this stage. NaCl particles, *a priori* sieved to obtain particles with diameters in the range of 200–400 μm, were then added into the neat or the drug-loaded solutions at four different NaCl to PBSu–DCH weight ratios (i.e., 25, 30, 35, and 40% w/w). The pasty suspensions were homogenized and a volume of the suspensions was filled with slight pressing in homemade cylindrical glass molds and Petri dishes to obtain molding samples of two different shapes and dimensions. The moldings were placed in a fume hood overnight to allow evaporation of the solvent. NaCl particles were then leached out by immersing the moldings in deionized (DI) water for 48 h, with DI water being replaced every 8 h. The obtained scaffolds were dried *in vacuo* at room temperature for 24 h. Hereafter, the scaffolds that were prepared with the NaCl to PBSu–DCH weight ratios of 25, 30, 35, and 40% w/w were denoted as 25×, 30×, 35×, and 40 × NaCl scaffolds, respectively. The dimension of the scaffolds obtained from the moldings cast in the homemade cylindrical glass molds (hereafter, cylindrical scaffolds) was 11.3 ± 0.2 mm in diameter and 8.6 ± 0.3 mm in height, while the moldings cast in the Petri dishes were later cut into a desired shape and size for further uses. Examples of the as-prepared scaffolds are available as Supplementary data (see Fig. II).

2.3. Characterization

2.3.1. Microstructure observation

One cylindrical scaffold was randomly selected from each group of samples. It was cut into pieces along both the longitudinal and the transverse directions. The cut pieces were mounted on copper stubs, coated with gold using a JEOL JFC-1100 sputtering device, and observed for their microscopic structure using JEOL JSM-5200 scanning electron microscopy (SEM).

2.3.2. Porosity, pore volume, and pore size

Porosity and pore volume of the scaffolds were measured gravimetrically according to the following equations:

$$\text{Porosity}(\%) = (1 - \rho_{\text{scaffold}}/\rho_{\text{polymer}}) \times 100 \quad (1)$$

$$\text{Pore volume}(\%) = (1/\rho_{\text{scaffold}} - 1/\rho_{\text{polymer}}) \times 100 \quad (2)$$

where ρ_{polymer} is the density of the polymer from which the scaffolds were fabricated and ρ_{scaffold} is the apparent density of the scaffolds which was measured by a Sartorius YDK01 density measurement kit. Here, $\rho_{\text{PBSu–DCH}}$ was taken the value of 1.2 g cm^{-3}. Five specimens were measured for both the porosity and the pore volume and an average value for each property was calculated. On the other hand, pore size of the scaffolds was directly measured from SEM images, using a UTHSCSA Image Tool version 3.0 software. At least 25 pores for each of the cross- and the longitudinal sections (i.e., at least 50 pores in total) were measured and the average values for all of the scaffolds investigated were calculated.

2.3.3. Mechanical properties

Both tensile and compressive properties of the scaffolds were determined in their dry state with a Lloyd LRX universal testing machine using 500 N load cell at room temperature. For the tensile test, specimens ($50 \times 15 \times 3$ mm^3) were cut from the moldings that had been cast in the Petri dishes. The gauge length was 30 mm and the crosshead speed was 5 mm min^{-1}. For the compressive test, the cylindrical scaffolds were compressed at the crosshead speed of 1 mm min^{-1} until the specimens were ~70% deformed from their original height of ~8.6 mm. The tensile test was carried out in pentuplicate and the compressive test was in triplicate.

2.3.4. Water retention ability

The scaffold specimens, cut from the moldings that had been cast in the Petri dishes (circular shape with 15 mm in diameter and 3 mm in height), were first dried, weighed, and individually immersed in 10 mL of 10 mM phosphate buffer saline solution (PBS; pH 7.4) at room temperature. At a given time point, the specimens were taken out, blotted on a glass plate which was set at ~30° from a horizontal baseline for 5 s to remove excess water, and immediately weighed. The amount of water retained in the specimens was determined according to the following equation:

$$\text{Water retention}(\%) = [(W_w - W_d)/W_w] \times 100, \quad (3)$$

where W_d and W_w are the weight of the specimens before and after submersion in the medium, respectively. The experiment was carried out in pentuplicate and the measurements were carried out at different time intervals within a period of 30 d.

2.3.5. In vitro *degradation*

The cylindrical scaffolds were individually placed in 15 mL of PBS and conditioned at 37 °C in a water bath without shaking. The PBS medium was refreshed once in a week to maintain the buffer capacity of the medium. At a given time point, the scaffolds were removed, washed twice with DI water, and dried *in vacuo* for 24 h.

The remaining weight of the scaffolds was determined as the weight ratio based on the initial weight of the scaffolds, according to the following equation:

$$\text{Remaining weight}(\%) = W_t/W_o \times 100, \quad (4)$$

where W_o is the initial weight of the scaffolds in their dry state and W_t is the weight of the scaffolds after the degradation assay in their dry state. The experiment was carried out in triplicate. Any change in the microstructure of the scaffolds after the degradation assay was observed by SEM.

2.3.6. Cytotoxicity and cell/scaffold interaction

Mouse calvaria-derived, pre-osteoblastic cells (MC3T3-E1; ATCC CRL-2593) were cultured as a monolayer in minimum essential medium (MEM; Sigma–Aldrich, USA), supplemented with 10% fetal bovine serum (FBS; Biochrom, Germany), 1% L-glutamine (Invitrogen, USA) and a 1% antibiotic and antimycotic formulation [containing penicillin G sodium, streptomycin sulfate, and amphotericin B (Invitrogen Corp.)]. The cells were maintained at 37 °C in a humidified atmosphere containing 5% CO_2 and passaged once every 3–4 d.

Only the 35 × NaCl scaffolds were used in these studies. Cytotoxicity of the as-prepared scaffolds was evaluated by the indirect cytotoxicity method, using MC3T3-E1 as the reference cells. First, the extraction media were prepared by immersing the scaffold specimens, cut from the moldings that had been cast in the Petri dishes (circular shape with 15 mm in diameter and 3 mm in height), in 500 μL of serum-free medium (SFM; containing MEM, 1% L-glutamine, 1% lactalbumin, and 1% antibiotic and antimycotic formulation) for 24 h. Each of these extraction media was used in the indirect cytotoxicity evaluation. MC3T3-E1 were cultured in wells of a 24-well culture plate at 3×10^4 cells/well in serum-containing MEM for 16 h to allow cell attachment on the plate. The cells were then starved with SFM for 24 h, after which time the medium was replaced with an extraction medium. After 24 h of cell culturing in the extraction medium, a 3-(4,5-dimethylthiazol-2-yl)-2,5-diphenyl-tetrazolium bromide (MTT) assay was carried out to determine the viability of the cells. The experiment was carried out in quadruplicate.

The MTT assay is based on the reduction of the yellow tetrazolium salt to purple formazan crystals by dehydrogenase enzymes secreted from the mitochondria of metabolically active cells. The amount of purple formazan crystals formed is proportional to the number of viable cells. First, each culture medium was aspirated and replaced with 500 μL/well of MTT solution at 0.5 mg mL^{-1} for a 24-well culture plate. Secondly, the plate was incubated for 1 h at 37 °C. The solution was then aspirated and 1 mL/well of dimethylsulfoxide (DMSO) containing 125 μL/well of glycine buffer (pH 10) was added to dissolve the formazan crystals. Finally, after 5 min of rotary agitation, the absorbance of the DMSO solution at 540 nm was measured using a Thermospectronic Genesis10 UV/Visible spectrophotometer.

A primary evaluation for the cell/scaffold interaction was carried out by a direct morphological observation of MC3T3-E1 that had been seeded on the surface of the scaffold specimens. Specifically, the scaffold specimens, cut from the moldings that had been cast in the Petri dishes (circular shape with 15 mm in diameter and 3 mm in height), were put in wells of a 24-well culture plate and sterilized with 1 mL of 70% ethanol for 30 min. They were then washed with sterilized DI water twice and later immersed in MEM overnight. MC3T3-E1 were then seeded on the surfaces of the specimens at 3×10^4 cells/specimen in a minimum volume of the culture medium and were allowed to attach on the surfaces for 3 h prior to the addition of 1.5 mL/well of the culture medium. The cells were cultivated at 37 °C in a humidified atmosphere containing 5% CO_2 for 24 h, after which time morphology of the attached cells was observed by SEM. After removal of the culture medium, the cell-cultured scaffold specimens were rinsed with PBS twice and the cells were then fixed with 3% glutaraldehyde solution, which had been diluted from 50% glutaraldehyde solution (Electron Microscopy Science, USA) with PBS for 30 min. The specimens were then dehydrated in ethanol solutions of varying concentration (i.e., 30, 50, 70, 90, and 100%) for ~2 min at each concentration, further dried in 100% hexamethyldisilazane (HMDS; Sigma, USA) for 5 min, and later dried in air after the removal of HMDS. Finally, the specimens were mounted on SEM stubs, coated with gold, and observed by SEM. The examinations were performed on three randomly selected scaffold specimens.

2.3.7. Inclusion, content, and release of ipriflavone

A Thermo Nicolet Nexus® 670 Fourier-transformed infrared (FT-IR) spectrophotometer was used to obtain the FT-IR spectra using the KBr disk method in order to confirm the existence of ipriflavone in the drug-loaded scaffolds, while a Shimadzu 2550 UV–vis spectrophotometer (UV–vis) was used to determine the amount of the as-loaded drug in the scaffolds against a predetermined calibration curve for ipriflavone (see Fig. III in Supplementary data). In the latter, the drug-loaded scaffold specimens were completely dissolved in chloroform and the amount of the as-loaded ipriflavone was measured in triplicate at the maximum wavelength of 249 nm. In the drug release assay, the drug-loaded scaffold specimens, cut from the moldings that had been cast in the Petri dishes (circular shape with 15 mm in diameter and 3 mm in height), were immersed in 10 mL of PBS containing 0.15% w/v sodium dodecyl sulfate (SDS) [15] and incubated in a shaking water bath (50 rpm) at 37 °C. At a given time point, an amount of the buffer solution (hereafter, the sample solution) was taken out and an equal amount of fresh medium was added in order to maintain a constant volume of the medium. The amount of the drug in the sample solution was determined spectrophotometrically at 249 nm. The experiment was carried out in triplicate.

2.3.8. Statistical analysis

Data were analyzed using the SPSS software version 14.0 for window. Initially, the normal distribution was assessed by the Shapiro–Wilk test. The normal distribution data, representing the homogeneity of the variances, shown by the Levene's test, were then investigated by the one way analysis of variance (ANOVA) with the Tukey HSD post-hoc multiple comparisons. Otherwise, the Dunnett T3 would be applied if the data did not exhibit the homogeneity of the variances. For the data of which the normal distribution was absent but the variance was homogeneous, the Kruskal–Wallis H test was applied. To compare the means between two data groups, the student's unpaired *t*-test was used. The significant level was indicated at $p < 0.05$ in any case.

3. Results

3.1. Microstructure observation

Selected SEM images illustrating microstructure of the as-prepared scaffolds when being viewed on the surface perpendicular to the longitudinal direction are shown in Fig. 1, while those illustrating the microstructure of the scaffolds when being viewed on the surface perpendicular to the transverse direction are available as Supplementary data (i.e., Fig. IV). For any given type of the scaffolds, there was no significant difference in the microstructure observed along both directions. On the other hand, marked difference in the microstructure of the scaffolds was observed with increasing the porogen content from 25 to 40% w/w. Specifically, at 25% w/w, a well-defined cubical porous structure, with the polymer

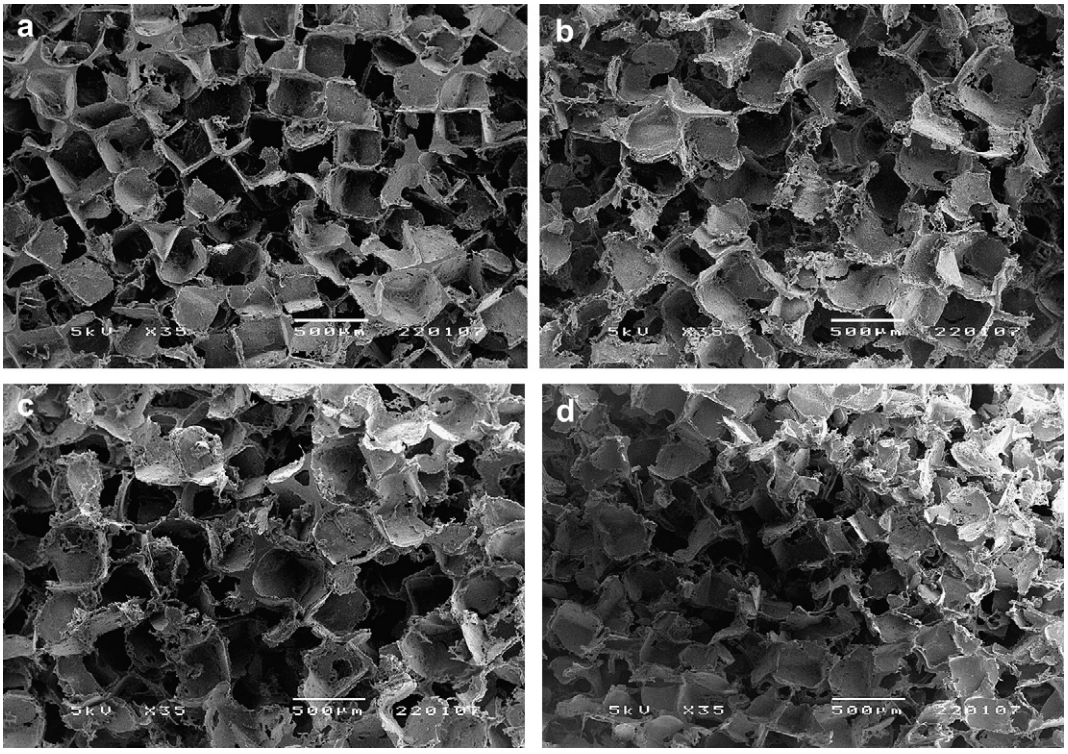

Fig. 1. Selected SEM images illustrating microstructure of the as-prepared PBSu–DCH scaffolds, i.e., (a) 25×, (b) 30×, (c) 35×, and (d) 40 × NaCl scaffolds, when being viewed on the surface perpendicular to the longitudinal direction (i.e., cross-sections).

mass conforming to the cubic particles of NaCl used in the fabrication process, was evident. Further increasing the porogen content to 30 and 35% w/w was responsible for the ill-defined cubical porous structure observed. At 40% w/w, most of the cubical compartments were substituted with the flake-liked structure. An increase in the porogen content from 25 to 40% w/w should be responsible for the observed increase in the inter-pore connectivity of the scaffolds.

3.2. Physical and mechanical characteristics

The as-prepared scaffolds were further characterized for their porosity, pore volume, and pore size (see Table 1). Significant increase in the property values was observed for the scaffolds that had been prepared with the porogen content ranging between 25 and 35% w/w, while such values for the scaffolds that had been prepared with the porogen contents of 35 and 40% w/w were statistically the same. Specifically, the porosity increased from ~94% for the 25 × NaCl scaffolds to ~96% for the 35× and the 40 × NaCl scaffolds; the pore volume increased from ~12 $cm^3 g^{-1}$ for the 25 × NaCl scaffolds to ~20 $cm^3 g^{-1}$ for the 35× and the 40 × NaCl scaffolds; and, finally, the pore size increased from ~297 μm for the 25 × NaCl scaffolds to ~379–408 μm for 35× and 40 × NaCl scaffolds. Clearly, the pore size was in the same range of the porogens used (i.e., 200–400 μm). The increase in the porosity of the scaffolds with increasing the porogen content resulted in an observed decrease in both the tensile and the compressive properties (see Table 2). Specifically, the compressive modulus decreased from ~55 kPa for the 25 × NaCl scaffolds to ~35 kPa for the 40 × NaCl scaffolds; the compressive strength decreased from ~16 kPa for the 25 × NaCl scaffolds to ~12 kPa for the 40 × NaCl scaffolds; the tensile modulus decreased from ~719 kPa for the 25 × NaCl scaffolds to ~164 kPa for the 40 × NaCl scaffolds; and, finally, the tensile strength decreased from ~62 kPa for the 25 × NaCl scaffolds to ~20 kPa for the 40 × NaCl scaffolds.

Table 1
Porosity, pore volume, and pore size of the as-prepared PBSu–DCH scaffolds

Sample	Porosity* (%)	Pore volume** ($cm^3 g^{-1}$)	Pore size** (μm)
25 × NaCl	93.96 ± 0.24^a	11.97 ± 0.51^a	296.7 ± 47.0^a
30 × NaCl	94.75 ± 0.24^b	13.91 ± 0.67^b	331.7 ± 66.1^b
35 × NaCl	96.20 ± 0.31^c	19.58 ± 1.66^c	378.9 ± 55.8^c
40 × NaCl	96.27 ± 0.14^c	19.90 ± 0.74^c	407.8 ± 69.5^c

[a,b,c] are significantly different at $p < 0.05$ for an individual feature; *one way ANOVA with Tukey HSD, **One way ANOVA with Dunnett T3; $n = 5$ for porosity and pore volume, $n = 50$ for pore size.

3.3. Water retention ability and in vitro degradability

The ability of a scaffold to absorb and retain exudates in its pore channels is a very important property of a functional scaffold in actual use, as exudates contain cells and various biological entities which are essential for tissue regeneration within the scaffold. Fig. 2 illustrates the ability of the as-prepared scaffolds in absorbing and retaining water in their porous structure after they had been immersed in PBS for various time intervals of up to 30 d (720 h) at room temperature. Among the various groups of the scaffolds, the 40 × NaCl group exhibited the greatest level of water retention, while the other three groups showed statistically similar values. All groups of the scaffolds demonstrated a similar water retention profile, i.e., an abrupt increase in the level of water retention during the first 24 h (see Fig. V in Supplementary data) to attain an ultimate value at a long submersion time. Hydrolytic degradation of the scaffolds was evaluated in PBS over a submersion period of 11 weeks. Fig. 3 shows the remaining weight of the scaffolds after having been submerged in PBS for different time intervals. A slight decrease in the weight of the scaffolds was observed during 5–9

Table 2
Mechanical properties of the as-prepared PBSu–DCH scaffolds

Sample	Compessive modulus* (kPa)	Compressive strength* (kPa)	Tensile modulus* (kPa)	Tensile strength** (kPa)
25 × NaCl	54.75 ± 4.87^{a}	15.66 ± 1.15^{a}	719.4 ± 28.4^{a}	61.63 ± 3.67^{a}
30 × NaCl	$52.90 \pm 2.70^{a,b}$	15.24 ± 0.75^{a}	301.7 ± 40.2^{b}	38.27 ± 3.44^{b}
35 × NaCl	47.17 ± 2.34^{b}	13.30 ± 0.71^{b}	240.5 ± 20.1^{c}	36.51 ± 1.98^{b}
40 × NaCl	35.17 ± 4.26^{c}	11.94 ± 1.13^{b}	163.6 ± 36.9^{d}	20.17 ± 1.62^{c}

*At 20% strain; **At rupture; ^{a,b,c,d} are significantly different at $p < 0.05$ for an individual feature; one way ANOVA with Tukey HSD.

weeks, while an abrupt decrease in their weight was observed during 9–11 weeks. The loss in the weight of these scaffolds at week 11 was an obvious increasing function of the porosity, despite no statistical difference among the four data groups. Morphological changes of the scaffolds after hydrolytic degradation were also studied by SEM (see Fig. VI in Supplementary data). Despite the observation of the irregular perforations at some thin parts of the cellular structure, which could be a strong evidence for the hydrolytic decomposition of these scaffolds in the basic medium, the overall porous architecture (i.e., porosity and pore size) of these scaffolds, for the most parts, was retained.

3.4. Cytotoxicity and cell/scaffold interaction

Cytotoxicity of the 35 × NaCl scaffolds was assessed by observing the relative viability of MC3T3-E1 that had been cultured with the extraction media from the scaffolds against that of the cells that had been cultured with SFM for 24 h (see Table 3). Evidently, the viability of the cells that had been cultured with either the extraction media or SFM was statistically the same, a result indicating that the as-prepared PBSu–DCH scaffolds are biocompatible to the bone cells. The non-toxicity of the scaffolds towards the bone cells was also confirmed with lactate dehydrogenase (LDH) cytotoxicity assay (see the additional experiment in Supplementary data). Further preliminary evaluation for the potential use of the scaffolding materials as supports for bone tissue regeneration was carried out by a direct seeding of the bone cells on the surfaces of the scaffolds. Fig. 4 shows selected SEM images of MC3T3-E1 that had been seeded on the surfaces of the 35 × NaCl scaffolds for 24 h. More images are also available as Supplementary data (see Fig. VII). Evidently, the cells adhered well on the surface of the scaffolds, with an evidence of cytoplasmic expansion of the cells over the surfaces. Though not shown, further examination of the underlying pores of the scaffolds showed an evidence of MC3T3-E1 that were migratory to the inner-side of the pores.

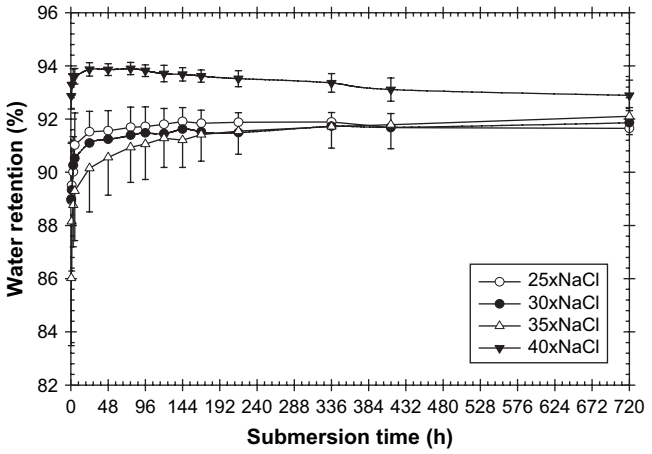

Fig. 2. Water retention ability of the as-prepared PBSu–DCH scaffolds that had been submerged in 10 mM PBS at room temperature as a function of submersion time.

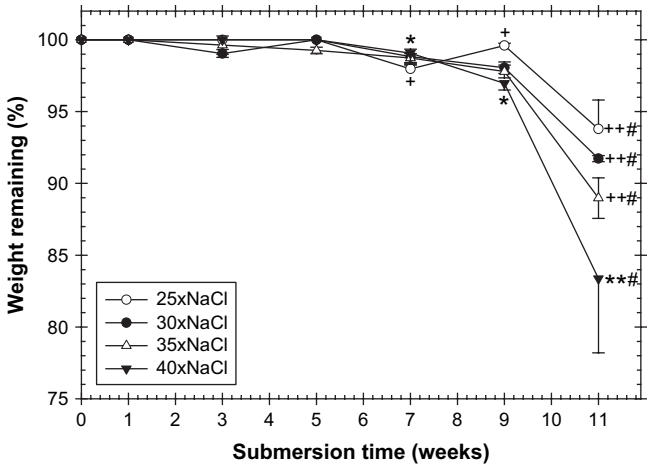

Fig. 3. Weight of the as-prepared PBSu–DCH scaffolds that remained after submersion in 10 mM PBS for various submersion times. $^{*}p < 0.05$, $^{+}p < 0.05$; one way ANOVA with Dunnett T3; $^{\#}p < 0.05$; Kruskal–Wallis H test.

3.5. Inclusion, content, and release of ipriflavone

The existence of ipriflavone in the ipriflavone-loaded PBSu–DCH scaffolds was investigated by FT-IR. Fig. 5 shows FT-IR spectra of the drug-loaded scaffolds in comparison with those of the pure constituents. In addition to the band characteristic to the ester bonds at 1724 cm^{-1}, the spectra showed the intense bands belonging to the carbonyl groups conjugated with an aromatic compound at 1636 and 1562 cm^{-1} (indicated by the broken arrows) and those of hydroxyl groups at 1260 cm^{-1} (indicated by the solid arrows) [16], which are absent from that of the neat PBSu–DCH scaffolds (viz. the FT-IR spectra of the different types of the neat scaffolds were identical). The amount of ipriflavone that had been loaded in the PBSu–DCH scaffolds was reported as either the actual amount of the loaded drug divided by the initial amount of drug loaded (i.e., 10% based on the weight of the polymer; hereafter, the loading efficiency) or the actual amount of the loaded drug divided by the weight of the scaffold specimens (hereafter, the loading capacity) (see Fig. 6). Evidently, the loading efficiency ranged between 69 and 87%, with a statistical difference being observed between the 25× and the 40 × NaCl groups. On the other hand, the loading capacity ranged between 75 and 86%, with no statistical difference among the various groups.

The release characteristic of ipriflavone from the drug-loaded PBSu–DCH scaffolds was carried out in a SDS-containing PBS solution at 37 °C for a total releasing period of 91 d. The actual amount of the as-loaded ipriflavone in the scaffolds was used to calculate the cumulative amount of the drug released from the

Table 3
Indirect cytotoxicity evaluation of the as-prepared 35 × NaCl scaffolds using mouse calvaria-derived, pre-osteoblastic cells (MC3T3-E1)

Sample no.	Absorbance at 540 nm	
	Control group	Experimental group
1	0.094	0.118
2	0.123	0.138
3	0.147	0.116
4	0.114	0.110
Average	0.119 ± 0.022^{a}	0.120 ± 0.012^{a}

[a] $p < 0.05$ significant level; Student's unpaired *t*-test.

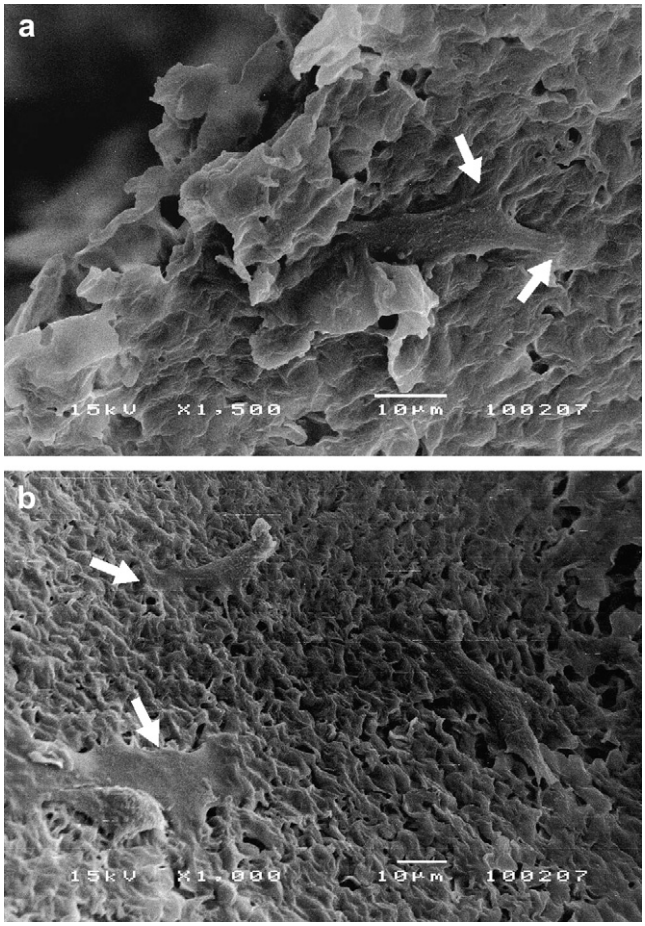

Fig. 4. Selected SEM images illustrating the morphology of MC3T3-E1 that were seeded on the surface of the 35 × NaCl scaffolds for 24 h. White arrows show the cytoplasmic edge of the cells.

drug-loaded scaffolds, as shown in Fig. 7. Evidently, all of the drug releasing profiles were identical in their appearance, which could be divided into two phases. Phase 1 correlated to an initial burst release of ipriflavone from the scaffolds which occurred within the first 24 h, while phase 2 corresponded to the sustained release of the drug (i.e., day 1–60) and the gradual decrease in the rate of the drug release to finally reach a plateau value (i.e., after day 70). Among the various groups, the cumulative amount of ipriflavone released from the 25 × NaCl scaffolds at any given time point was the lowest (with the total amount of the drug released on day 91 being ~55%), while those released from all other groups were statistically the same (with the total amount of the drug released on day 91 being in the range of ~69–71%).

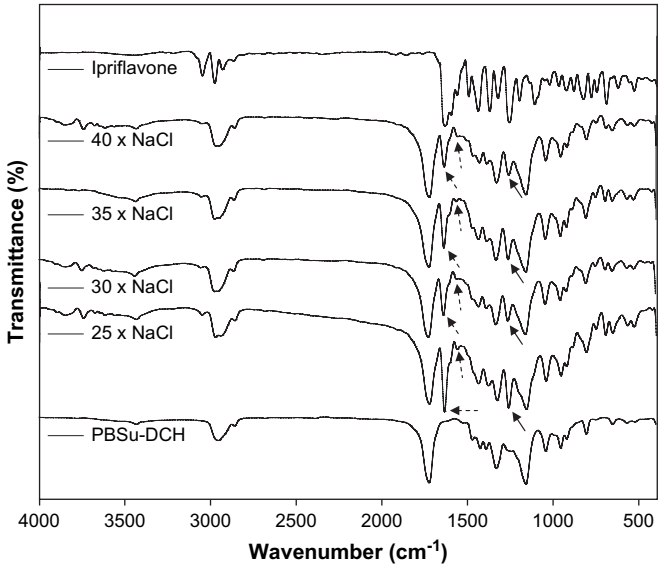

Fig. 5. FT-IR spectra of the neat PBSu–DCH scaffolds, ipriflavone, and the ipriflavone-loaded PBSu–DCH scaffolds. FT-IR spectra for all of the neat scaffolds were the same, thus only the representative spectrum (i.e., denoted as PBSu–DCH) is shown.

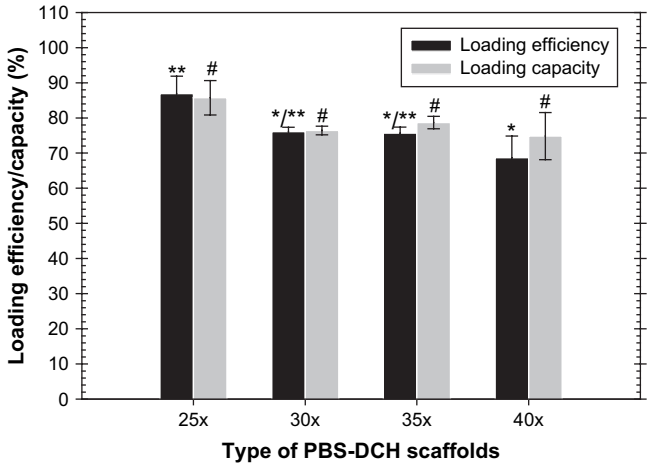

Fig. 6. Loading efficiency/capacity of ipriflavone in the ipriflavone-loaded PBSu–DCH scaffolds. $^{*}p < 0.05$, $^{\#}p < 0.05$; Kruskal–Wallis H test.

4. Discussion

4.1. Fabrication technique and scaffold characteristics

The particulate leaching technique has a number of advantages over the freeze–drying technique, based on the physico-chemical properties and cell-culturing benefits of the as-prepared porous scaffolds [17]. In this technique, the optimal micro-structural morphology, i.e., porosity and pore size, could be readily produced with the choice of an appropriate amount and size of the porogen particles used. Based on the porosity values and the observed inter-pore connectivity of the as-prepared PBSu–DCH scaffolds, the ones that were prepared at the NaCl to PBSu–DCH weight ratio of 30 and 35 showed the most satisfactory microstructure (see Fig. 1b and c),

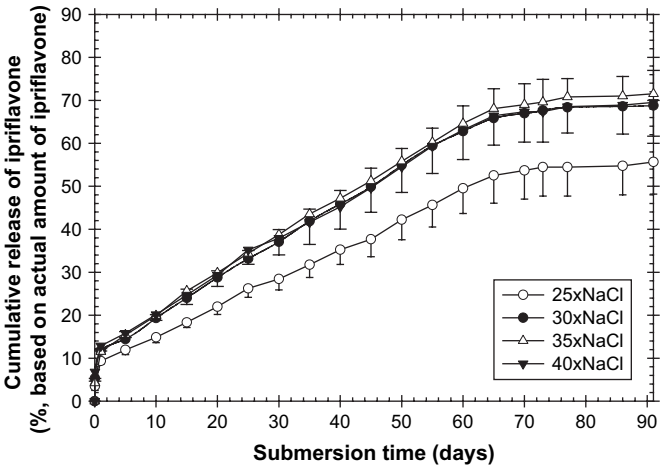

Fig. 7. Cumulative releasing profiles of ipriflavone from the ipriflavone-loaded PBSu–DCH scaffolds in a SDS-containing PBS solution at 37 °C.

while those prepared at the NaCl to PBSu–DCH weight ratio of 25 and 40 were unacceptable. Apparently, the microstructure of the scaffolds conformed to the way the NaCl particles accumulated and arranged themselves within the matrix. Large pores with either regular or irregular shape were created by disconnection of the matrix as spaces were occupied by the porogen particles. As presented in Table 1, the porosity, the pore volume, and the pore size significantly increased with an increase in the NaCl contents from 25 to 35% w/w. Between the NaCl contents of 35 and 40% w/w, the difference in the property values of the obtained scaffolds was statistically insignificant. At these contents, the amount of porogens may reach saturation in terms of their packing efficiency.

4.2. Physico-mechanical and biological properties

Variation in the microstructure, especially the pore features, of the scaffolds corresponded to their expressive physico-mechanical properties. From the mechanical standpoint, the tensile moduli of the as-prepared porous PBSu–DCH scaffolds (i.e., ~164–719 kPa) were much lower than that of the neat, melt-pressed PBSu films (i.e., ~0.5 GPa) [11]. Comparatively, the variation in the compressive property values among various sample groups was significantly narrower than that in the tensile counterparts (see Table 2). Despite the observed decrease in the mechanical property values with increasing the porosity or the pore size of the scaffolds, specific correlations between the property values and the porosity or the pore size could not be made. In addition, the obtained results indicated that the as-prepared scaffolds were able to withstand tension over compression. These two deformational modes will be introduced to a scaffold when it is placed in alveolar bone socket and, as an affidavit of its actual applicability, the as-prepared scaffolds were proven to be strong enough as they could be securely placed without any sign of rupture in the narrow captivity of the apical area of a micro-centrifugal tube.

Water retention ability of a porous scaffold is an indispensable factor determining its actual utilization, as it allows the absorption and retention of blood in the porous structure of the scaffold. Normally, retention of blood leads to thrombosis, which is one of the steps required for bone regeneration. Water retention ability of the porous scaffold depends significantly on the chemical property of the fabricated material as well as the porosity and the architecture of the porous structure (i.e., pore volume and pore size) [18]. According to the results shown in Table 1 and Figs. 1 and 2, the greatest porosity, pore volume, and pore size values and the highest inter-pore connectivity observed for the 40 × NaCl scaffolds are the obvious reasons for their greatest water retention ability. Nevertheless, after 1 h of submersion in PBS, the water retention value for all types of the scaffolds ranged between 88 and 93%, while, after 24 h of submersion, it ranged between 90 and 94%. Obviously, these scaffolds exhibited relatively high water retention ability.

High water retention ability is also a condition in favor of hydrolytic degradation of the scaffolds. Here, the hydrolytic degradation of the as-prepared PBSu–DCH scaffolds was studied by evaluating any change in the weight of the materials as a responsive indicator [19]. According to the results shown in Fig. 3, the weights of the 25×, 30×, 35×, and 40 × NaCl scaffolds that remained after having been submerged in PBS for 11 weeks were ~94, ~92, ~89, and ~83% of their initial weights, respectively. As previously noted, the hydrolytic degradation of the scaffolds after submersion in PBS for 11 weeks was also visualized by SEM (see Fig. VI in Supplementary data), in which decomposition of the materials was observed on the flat surfaces of inter-cellular walls. Despite the evidence of the hydrolytic degradation, physical integrity of the scaffolds was maintained throughout the 11-week period of the investigation. Particularly, there was no sign of significant degradation during the first 2 months. This time period is concomitant with sequential stages during the proliferation and differentiation of bone cells, including proliferation, bone matrix formation and maturation, and mineralization [20], after which time the scaffolds will finally vanish to provide space for the newly-growing bone tissue [7].

Factually, biodegradation of a polymer is a multi-factorial behavior. Both the degree of crystallinity and the stiffness of the molecular chains were known to be influential in the degradation of PBSu and its co-polymers [12,13]. The theoretical crystallinity of PBSu–DCH, used in this study, was 49.7%. This value was calculated from the ratio of the apparent enthalpy of fusion of this material (i.e., 54.9 J g^{-1}) to the theoretical value for a perfectly crystalline PBSu (i.e., 110.5 J g^{-1}), which was determined based on the group contribution basis [13]. Extending PBSu with hexamethylene diisocyanate makes the polymer chains longer and more flexible, which should adversely affect the crystallization of the resulting polymer and, at the same time, increases its degradation susceptibility. Hence, it seems logical to postulate that the degradation of the as-prepared porous PBSu–DCH scaffolds was enhanced by both the chemical characteristic of the fabricated material and the observed high water retention ability of the scaffolds.

The legitimacy in the use of the as-prepared porous materials as bone scaffolds was assessed by evaluating their cytotoxicity and ability to support the attachment of MC3T3-E1. The 35 × NaCl scaffolds were chosen for such evaluations, due to the balance in their pore architecture, mechanical integrity, and biodegradability. High porosity and large pore sizes encourage *in vivo* bone formation [21–23] and the pore sizes greater than ~300 μm were optimal to facilitate vascularization and direct bone formation without preceding cartilage formation [24]. On the other hand, when the porosity and the pore sizes are too great, the resulting scaffolds may become too weak and degrade too fast, such that their *in vivo* applicability cannot be realized. The 35 × NaCl scaffolds were then chosen as a result. Both the indirect and the LDH cytotoxicity evaluations showed that the PBSu–DCH scaffolds were biocompatible to the osteoblast-like cells. Selected SEM images also revealed satisfactory cell/scaffold interaction, as MC3T3-E1 adhered well on the scaffold surfaces. Certain cells showed their flat bodies and broad lamellipodia, indicating that the cell cortex was under tension due to the motility process [25]. Since the ability of mammalian cells to attach on a surface influences their capacity to proliferate and differentiate [26,27], the as-prepared porous materials could be used as functional bone scaffolds.

4.3. Release characteristic of ipriflavone

The potential for use of the as-prepared porous PBSu–DCH materials as effectual drug-releasing porous scaffolds was evaluated using ipriflavone, known for its bone regenerative activity, as the model drug. Both the porosity and the pore size seemed to have little effect on the incorporation of the drug within the scaffolds, as both the loading efficiency and the loading capacity of the drug in the scaffolds were high. Irrespective to the statistical analysis, the 25 × NaCl scaffolds exhibited the greatest loading efficiency and the loading capacity on average. This could be a result of the unequal weight of the scaffold specimens used to determine the amount of the as-loaded drug, as the fabrication of the scaffolds was on the iso-volumetric basis. As a result, the weight of the 25 × NaCl scaffold specimens was the greatest, due to the greatest amount of the polymer mass. The highest polymer mass translated to the greatest possibility for drug incorporation, as observed.

The *in vitro* release of ipriflavone from the salt-leached, porous PBSu–DCH scaffolds was completed in ~2 months. The initial burst

release of the drug within the first 24 h should be caused by the dissolution of some kinds of drug aggregates that were observed on the superficial cellular surfaces of the scaffolds (results not shown) into the dissolution medium [15]. Clearly, the sustained release of the drug in phase 2 (during day 1–60) with a constant rate of release (i.e., $\sim 0.64\% \, d^{-1}$ for the $25 \times$ NaCl scaffolds and ~ 0.84–$0.88\% \, d^{-1}$ for the rest of the scaffolds) was the outstanding feature of these scaffolds. Such time frame unexpectedly matches with the period required for both the proliferation and the differentiation of the bone cells [7,20] without a noticeable loss in the mass the scaffolds due to degradation (see Fig. 3). Interestingly, only the $25 \times$ NaCl scaffolds showed the lowest amount of cumulative release of ipriflavone, while all other groups showed an almost identical releasing profiles of the drug. This, again, could be due to the fact that the weight of the $25 \times$ NaCl scaffold specimens was the greatest, causing the inter-cellular walls to be thicker than those of the other scaffolds. The thicker inter-cellular walls should greatly influence the diffusion of the drug from the matrix. Nonetheless, other factors, i.e., different loading capacity of the drug within these different scaffolds, could also play a role.

5. Conclusion

Poly(1,4-butylene succinate) extended with 1,6-diiocyanatohexane (PBSu–DCH) was successfully fabricated into porous scaffolds by solvent casting and particulate leaching technique, using sodium chloride (NaCl) particles as the leachable component (i.e., porogens). The microstructure of the scaffolds can be tailored by varying the amount of the porogens (i.e., 25, 30, 35, and 40% based on the weight of PBSu–DCH). The porosity, pore volume, pore size, and inter-pore connectivity hypothetically increased, while both the tensile and the compressive strength and modulus hypothetically decreased, with increasing the porogen content. The suitability of the as-prepared porous materials as bone scaffolds was confirmed by their ability to absorb and retain water quickly even after 1 h after submersion in the phosphate buffer saline solution (PBS; pH 7.4), the negative results on the cytotoxicity evaluation, and their ability to support the attachment of mouse calvaria-derived, pre-osteoblastic cells (MC3T3-E1) that had been seeded on their surfaces for 24 h. The potential for use of the as-prepared porous materials as effectual drug-releasing scaffolds was assessed with ipriflavone as the model drug. Interestingly, the release of ipriflavone from the drug-loaded porous scaffolds was completed in ~ 2 months, with sustained release of the substance being observed during day 1–60. Based on these results, the salt-leached, porous PBSu–DCH scaffolds serve well as alternative biomaterials for bone tissue regeneration, particularly in dental sockets where load-bearing functionality is not of prime concern.

Acknowledgments

The authors acknowledged partial support received from (a) the National Center of Excellence for Petroleum, Petrochemicals, and Advanced Materials (NCE-PPAM), and (b) the Petroleum and Petrochemical College (PPC), Chulalongkorn University.

Appendix. Supplementary data

Supplementary data associated with this article can be found in the online version, at doi:10.1016/j.polymer.2008.04.006.

References

[1] Bodic F, Hamel L, Lerouxel E, Baslé MF, Chappard D. Joint Bone Spine 2005; 72:215.
[2] Jahangiri L, Devlin H, Ting K, Nishimura I. J Prosthet Dent 1998;80:224.
[3] Wiesen M, Krtzis R. Periodontal Clin Investig 1998;20:17.
[4] Hanne E, Sonis S, Gallagher G, Adwood D. J Prosthet Dent 1988;60:729.
[5] Altundal H, Gűvener Ő. Int J Oral Maxillofac Surg 2004;33:286.
[6] Yaffe A, Binderman I, Breuer E, Pinto T, Golomb G. J Periodontol 1999;70:893.
[7] Hutmacher DW. Biomaterials 2000;21:2529.
[8] Drotleff S, Lungwitz U, Breunig M, Dennis A, Blunk T, Tessmar J, et al. Eur J Pharm Biopharm 2004;58:385.
[9] Wiesmann HP, Meyer UJ. Int J Oral Maxillofac Surg 2004;33:523.
[10] Griffith LG. Acta Mater 2000;48:263.
[11] Li H, Chang J, Cao A, Wang J. Macromol Biosci 2005;5:433.
[12] Nikolic MS, Poleti D, Djonlagic J. Eur Polym J 2003;39:2183.
[13] Nikolic MS, Djonlagic J. Polym Degrad Stab 2001;74:263.
[14] Civitelli R. Calcif Tissue Int 1997;61:S12.
[15] Perugini P, Genta I, Conti B, Modena T, Cocchi D, Zaffe D, et al. Int J Pharm 2003;256:153.
[16] Coates J. Interpretation of infrared spectra, a practical approach. Encyclopedia of analytical chemistry. Chichester: John Wiley & Sons Ltd; 2000. p. 10815.
[17] Lee SB, Kim YH, Chong MS, Hong SH, Lee YM. Biomaterials 2005;26:1961.
[18] Park SN, Park JC, Kim HO, Song MJ, Suh H. Biomaterials 2002;23:1205.
[19] Shishatskaya EI, Volvova TG, Gordeev SA, Puzyr AP. J Biomater Sci Polym Ed 2005;16:643.
[20] Wutticharoenmongkol P, Pavasant P, Supaphol P. Biomacromolecules 2007;8: 2602.
[21] Roy TD, Simon JL, Ricci JL, Rekow ED, Thompson VP, Parsons JR. J Biomed Mater Res A 2003;66:283.
[22] Lewandrowski KU, Gresser JD, Bondre S, Silva AE, Wise DL, Trantolo DJ. J Biomater Sci Polym Ed 2000;11:879.
[23] Kuboki Y, Jin Q, Kikuchi M, Mamood J, Takita H. Connect Tissue Res 2002;43: 529.
[24] Jin QM, Takita H, Kohgo T, Atsumi K, Itoh H, Kuboki Y. J Biomed Mater Res 2000;51:491.
[25] Alberts B, Johnson A, Lewis J, Raff M, Roberts K, Walter P. Molecular biology of the cell. 4th ed. New York: Garland Science; 2002. p. 972.
[26] Anselme K. Biomaterials 2000;21:667.
[27] Sittinger M, Hutmacher DW, Risbud MV. Curr Opin Biotechnol 2004;15:411.